

Ridges and Ravines on Implicit Surfaces

Alexander G. Belyaev
The University of Aizu
Aizu-Wakamatsu City
Fukushima 965-8580 Japan
belyaev@u-aizu.ac.jp

Alexander A. Pasko
The University of Aizu
Aizu-Wakamatsu City
Fukushima 965-8580 Japan
pasko@u-aizu.ac.jp

Tosiyasu L. Kunii
Hosei University
3-7-2 Kajino-cho Koganei City
Tokyo 184-0002 Japan
tosi@kunii.com

Abstract

Surface creases provide us with important information about the shapes of objects and can be intuitively defined as curves on a surface along which the surface bends sharply. Our mathematical description of such surface creases is based on study of extrema of the principal curvatures along their curvature lines.

On a smooth generic surface we define ridges to be the local positive maxima of the maximal principal curvature along its associated curvature line and ravines to be the local negative minima of the minimal principal curvature along its associated curvature line. The ridges and ravines are important for shape analysis and possess remarkable mathematical properties. For example, they correspond to the end points of shape skeletons.

In this paper we derive formulas to detect the ridges and ravines on a surface given in implicit form. We also propose an algorithm of obtaining piecewise linear approximation of ridges and ravines as intersection curves of two implicit surfaces.

Introduction

Surface creases provide us with important information about the shapes of objects and can be intuitively defined as curves on a surface along which the surface bends sharply. Our mathematical description of surface creases is based on study of extrema of the principal curvatures along their curvature lines. Besides the mathematical beauty of such surface features [16], they have been studied in connection with applications in image and data analysis [21, 7], face recognition [8], quality control of free-form surfaces [9], analysis of medical images [4, 5, 14, 19] and satellite data [13]. See also references therein. Shape description with curvature extrema has been a subject of research in [12, 10].

Let us briefly recall here basic notions of differential geometry required for our study. Consider a plane passing

through a point \mathbf{p} in a given oriented surface M and normal to the surface. We call the intersection curve by the *normal section curve*. The curvature of the normal section curve depends on its tangent vector at \mathbf{p} . The maximal and minimal curvatures k_{\max} and k_{\min} are called the *principal curvatures* of M at \mathbf{p} . The associated tangent directions \mathbf{t}_{\max} and \mathbf{t}_{\min} are called the *principal directions* of M at \mathbf{p} . The integral curves of the principal direction fields are called the *curvature lines*. A point at which one of the principal curvatures vanishes is called *parabolic*. A point at which the principal curvatures are equal to each other is called *umbilic*. The *principal centers of curvature* are the points situated on the surface normal passing through \mathbf{p} at distances k_{\max}^{-1} and k_{\min}^{-1} from \mathbf{p} . The loci of the principal centers form the *caustic*. The caustic consists of two sheets corresponding to the maximal and minimal principal curvatures.

Definition 1 A non-umbilic point $\mathbf{p} \in M$ is called a *ridge point* if k_{\max} attains a local positive maximum at \mathbf{p} along the associated curvature line. A non-umbilic point $\mathbf{q} \in M$ is called a *ravine point* if k_{\min} attains a local negative minimum at \mathbf{q} along the associated curvature line.

Remark 1 Although in this definition we deal with non-umbilic points the umbilics can be treated by continuity.

Remark 2 The definitions of the ridges and ravines are dual: if we change the surface orientation then the ridges turn into the ravines and vice versa. Without loss of generality we can consider only the ridges.

Remark 3 In the mathematical part of our research we deal with generic phenomena. Roughly speaking, a particular property of an object from a particular class of objects is generic if in the space of all the objects of that class the objects exhibiting the property form an open dense set.

It turns out [1, 2] that the ridges and ravines are closely connected with shape skeletons and caustic singularities.

- The cuspidal edges of the caustic sheet associated with the maximal principal curvature and pointing towards to the surface correspond to the ridges.
- The boundary points of the singularities of the distance function from a generic smooth oriented surface correspond to ridge and ravine points. In particular the boundary points of the 3D Blum skeleton of a generic closed smooth surface oriented by its inward normal correspond to ridge points. Close results were obtained in [22, 17].
- The ridges do not pass through the generic umbilics. Therefore the ridges does not contain branch points. Close results can be found in [16, 11].

These remarkable properties are schematically illustrated by Fig. 1.

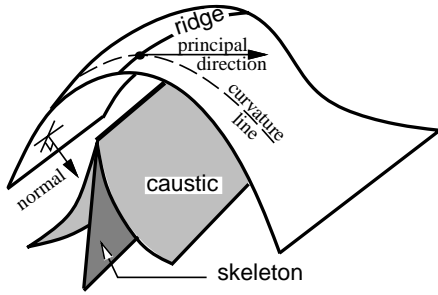


Figure 1.

In this paper we derive formulas to detect the ridges and ravines on a surface given in implicit form. We also propose an algorithm of obtaining piecewise linear approximation of ridges and ravines as intersection curves of two implicit surfaces.

The proposed approach can be also extended to treat a surface given in parametric form. However for parametric surfaces it seems better to extract the principal curvature extrema along the associated curvature lines while tracing the lines by differential equation solving (see [9, 10] for practical methods to trace the curvature lines).

Local analysis of ridge and ravine points

Let M be a given smooth generic surface. Denote by k_{\max} and k_{\min} the largest and the smallest principal curvatures respectively. For a given non-umbilic point $\mathbf{p} \in M$ let us choose coordinates in the space so that \mathbf{p} is at the origin, the (x, y) -plane is the tangent plane to the surface at \mathbf{p} , and the principal directions coincide with x and y axes. Then the surface is expressible in the Monge form as the graph of

a generic smooth function $z = f(x, y)$, where

$$f(x, y) = \frac{1}{2}(\lambda x^2 + \mu y^2) + \frac{1}{6}(ax^3 + 3bx^2y + 3cxy^2 + dy^3) + \frac{1}{24}(ex^4 + \dots) + O(x, y)^5$$

with $\lambda = k_{\max}(0, 0)$, $\mu = k_{\min}(0, 0)$, $\lambda > \mu$.

The Taylor series expansion of k_{\max} at \mathbf{p} has the form

$$k_{\max}(x, y) = \lambda + ax + by + O(x, y)^2.$$

Since the vectors $(1, 0)$ and $(0, 1)$ represent \mathbf{t}_{\max} and \mathbf{t}_{\min} at \mathbf{p} respectively, then

$$\frac{\partial k_{\max}}{\partial \mathbf{t}_{\max}} = a, \quad \frac{\partial k_{\max}}{\partial \mathbf{t}_{\min}} = b. \quad (1)$$

Let the surface orientation be chosen so that the maximal principal curvature is strictly positive at \mathbf{p}

$$k_{\max}(0, 0) > 0.$$

The curvature line associated with k_{\max} is locally described by the problem

$$\frac{dy}{dx} = \frac{bx + cy}{\lambda - \mu} + O(x, y)^2, \quad y(0) = 0.$$

Therefore

$$y'(0) = 0, \quad y''(0) = \frac{b}{\lambda - \mu}$$

and in a neighborhood of the origin the curvature line is approximated by the parabola

$$y = \frac{bx^2}{2(\lambda - \mu)}.$$

It allows to compute the Taylor series expansion of k_{\max} at the origin along the associated curvature line [1, 2]

$$\lambda + ax + \left(-3\lambda^3 + e + \frac{3b^2}{\lambda - \mu}\right) \frac{x^2}{2} + O(x^3) \quad (2)$$

Analyzing asymptotic expansion (2) we obtain that \mathbf{p} is a generic ridge point iff

$$a = 0 \quad \text{and} \quad -3\lambda^3 + e + \frac{3b^2}{\lambda - \mu} < 0. \quad (3)$$

Let us now consider a plane containing x axis: $\{y = \alpha z\}$, where α is a parameter. The intersection curve between the surface and the plane is locally described by the equation $y = \alpha \lambda x^2 / 2 + \dots$. The Taylor expansion of k_{\max} at the origin along the intersection curve has the form

$$\lambda + ax + \left(-3\lambda^3 + e + \frac{2b^2}{\lambda - \mu} + b\lambda\alpha\right) \frac{x^2}{2} + O(x^3) \quad (4)$$

If the plane is the normal section then $\alpha = 0$. Thus the points where k_{\max} takes a local positive maximum along the associated normal sections are characterized by the conditions

$$a = 0 \quad \text{and} \quad -3\lambda^3 + e + \frac{2b^2}{\lambda - \mu} < 0. \quad (5)$$

Denote by s_{\max} and s_{\min} arclength parameters of the normal sections associated with \mathbf{t}_{\max} and \mathbf{t}_{\min} respectively. Denote also by l_{\max} and l_{\min} arclength parameters of the curvature lines associated with \mathbf{t}_{\max} and \mathbf{t}_{\min} respectively. Taking into account (1), (2), and (4) with $\alpha = 0$ we get

$$\frac{d^2 k_{\max}}{dl_{\max}^2} = \frac{d^2 k_{\max}}{ds_{\max}^2} - \frac{1}{(k_{\max} - k_{\min})} \left(\frac{dk_{\max}}{ds_{\min}} \right)^2. \quad (6)$$

Formula (6) reduces calculation of the second derivative of the maximal principal curvature along its curvature line to the second derivative of the curvature along the corresponding normal section curve. For an implicit surface $F(x^1, x^2, x^3) = 0$ a formula for the latter will be obtained in the next section (formula (12)).

Surface in implicit form

Let now M be given in implicit form

$$F(x^1, x^2, x^3) = 0 \quad (7)$$

We use upper indices for vector components, subindices for partial derivatives with respect to x^i , $i = 1, 2, 3$, and Einstein summation convention: identical indices that appear one up and one down are summed over. For example,

$$F_{ijl} t^i t^j t^l + 3k F_{ij} t^i n^j$$

means

$$\sum_{i=1}^3 \sum_{j=1}^3 \sum_{l=1}^3 \frac{\partial^3 F}{\partial x_i \partial x_j \partial x_l} t^i t^j t^l + 3k \sum_{i=1}^3 \sum_{j=1}^3 \frac{\partial^2 F}{\partial x_i \partial x_j} t^i n^j.$$

The components of the surface unit normal vector are given by $n^i = -F_i/g$, where $g = |\nabla F|$ is the absolute value of the gradient.

Let k , \mathbf{t} , and s stand for a principal curvature, the associated principal vector, and the arclength parameter along the associated normal section respectively.

According to the Frenet formulas we have at \mathbf{p}

$$\frac{d\mathbf{t}}{ds} = k\mathbf{n}, \quad \frac{d\mathbf{n}}{ds} = -k\mathbf{t}.$$

Differentiating $F_i t^i = 0$ with respect to s gives

$$\frac{d}{ds}(F_i t^i) = F_{ij} t^i t^j + k F_i n^i = F_{ij} t^i t^j - kg.$$

Thus the principal curvatures k is given by

$$k = \frac{F_{ij} t^i t^j}{g} \quad (8)$$

Note that

$$\frac{dg}{ds} = g_i t^i = \frac{F_{ij} t^i F_j}{g} = -F_{ij} t^i n^j.$$

Differentiating (8) with respect to s yields

$$\frac{dk}{ds} = \frac{d}{ds} \left(\frac{F_{ij} t^i t^j}{g} \right) = \frac{F_{ijl} t^i t^j t^l + 3k F_{ij} t^i n^j}{g}. \quad (9)$$

In particular

$$\begin{aligned} \nabla k_{\max} \cdot \mathbf{t}_{\max} &= \frac{dk_{\max}}{ds_{\max}} = \frac{dk_{\max}}{dl_{\max}} = \\ &= \frac{F_{ijl} t_{\max}^i t_{\max}^j t_{\max}^l + 3k F_{ij} t_{\max}^i n^j}{g} \end{aligned} \quad (10)$$

Similar calculations lead to

$$\begin{aligned} \frac{d^2 k}{ds^2} &= \frac{d}{ds} \left(\frac{F_{ijl} t^i t^j t^l + 3k F_{ij} t^i n^j}{g} \right) = \\ &= \frac{1}{g} \left(F_{ijlm} t^i t^j t^l t^m + 6k F_{ijl} t^i t^j n^l + \right. \\ &\quad \left. + 4 \frac{dk}{ds} F_{ij} t^i n^j + 3k^2 F_{ij} n^i n^j \right) - 3k^3. \end{aligned} \quad (11)$$

In particular

$$\begin{aligned} \frac{d^2 k_{\max}}{ds_{\max}^2} &= \frac{1}{g} \left(F_{ijlm} t_{\max}^i t_{\max}^j t_{\max}^l t_{\max}^m + \right. \\ &\quad \left. + 6k_{\max} F_{ijl} t_{\max}^i t_{\max}^j t_{\max}^l n^l + 4 \frac{dk_{\max}}{ds_{\max}} F_{ij} t_{\max}^i n^j + \right. \\ &\quad \left. + 3k_{\max}^2 F_{ij} n^i n^j \right) - 3k_{\max}^3. \end{aligned} \quad (12)$$

Since

$$\begin{aligned} 0 &= \frac{d}{ds_{\min}} (\mathbf{t}_{\max} \cdot \mathbf{t}_{\max}) = 2 \frac{d\mathbf{t}_{\max}}{ds_{\min}} \cdot \mathbf{t}_{\max}, \\ 0 &= \frac{d}{ds_{\min}} (\mathbf{t}_{\max} \cdot \mathbf{t}_{\min}) = \frac{d\mathbf{t}_{\max}}{ds_{\min}} \cdot \mathbf{t}_{\min}, \\ 0 &= \frac{d}{ds_{\min}} (\mathbf{t}_{\max} \cdot \mathbf{n}) = \frac{d\mathbf{t}_{\max}}{ds_{\min}} \cdot \mathbf{n}, \end{aligned}$$

then $\frac{d\mathbf{t}_{\max}}{ds_{\min}} = 0$ and, therefore,

$$\begin{aligned} \frac{dk_{\max}}{ds_{\min}} &= \frac{d}{ds_{\min}} \left(\frac{F_{ij} t_{\max}^i t_{\max}^j}{g} \right) = \\ &= \frac{F_{ijl} t_{\max}^i t_{\max}^j t_{\min}^l + k_{\max} F_{ij} t_{\min}^i n^j}{g}. \end{aligned} \quad (13)$$

Formulas (8), (9), (10), and (13) can be found in [14, 16]. Formulas (6), (11), and (12) are new.

Theorem 1 *The generic ridge points are characterized by the conditions*

$$k_{\max} > 0, \quad \frac{dk_{\max}}{ds_{\max}} = 0, \quad \frac{d^2k_{\max}}{ds_{\max}^2} < 0, \quad (14)$$

where the first derivative of the maximal principal curvature along its associated curvature line is given by (10) and the second derivative is found from (6), (12) and (13).

In our practical computations of the principal curvatures and directions we follow [6]. Let us consider the matrix $-\nabla \mathbf{n}$ where the unit normal vector \mathbf{n} is given by $\mathbf{n} = -\nabla F / |\nabla F|$. Calculations show that

$$-\nabla \mathbf{n} = \frac{1}{|\nabla F|} (\mathbf{I} - \mathbf{n} \cdot \mathbf{n}^T) \mathbf{Hes}(F),$$

where \mathbf{I} is the identity matrix, $\mathbf{Hes}(F)$ is the Hessian of F , $[\mathbf{Hes}(F)]_{ij} = F_{ij}$, and $[\mathbf{n} \cdot \mathbf{n}^T]_{ij} = F_i F_j$. The matrix $-\nabla \mathbf{n}$ has the eigenvalues k_{\max} , k_{\min} , and 0 associated with the eigenvectors \mathbf{t}_{\max} , \mathbf{t}_{\min} , and \mathbf{n} respectively. Thus the characteristic polynomial $\det[\nabla \mathbf{n} + \lambda \mathbf{I}]$ of $-\nabla \mathbf{n}$ has the form $\lambda(\lambda^2 - 2H\lambda + K)$. It allows to represent the Gaussian and mean curvatures K and H in the following elegant form (see, for example, [20])

$$K = -\frac{1}{|\nabla F|^4} \det \begin{vmatrix} F_{11} & F_{12} & F_{13} & F_1 \\ F_{21} & F_{22} & F_{23} & F_2 \\ F_{31} & F_{32} & F_{33} & F_3 \\ F_1 & F_2 & F_3 & 0 \end{vmatrix}$$

$$H = \frac{1}{2|\nabla F|^3} \left(|\nabla F|^2 \Delta F - \sum_{i=1}^3 \sum_{j=1}^3 F_i F_j F_{ij} \right),$$

where Δ is the Laplacian. The principal curvatures are given by

$$k_{\max} = H + \sqrt{H^2 - K}, \quad k_{\min} = H - \sqrt{H^2 - K}.$$

In order to find the principal direction \mathbf{t}_{\max} let us consider the vectors obtained as the pairwise vector products of the rows of the matrix $[\nabla \mathbf{n} + k_{\max} \mathbf{I}]$. Now let us choose among them a vector of maximal norm and normalize it. We get \mathbf{t}_{\max} . The principal direction \mathbf{t}_{\min} is found as the vector product of \mathbf{t}_{\max} and \mathbf{n} .

Ridges and ravines as surface-surface intersection curves

As it was shown in the previous sections, ridges and ravines can be defined by systems of two non-linear equations and two inequalities.

The crucial step in our numerical extraction of the ridges and ravines is finding an intersection curve of two surfaces

given in implicit form (implicit surfaces): the initial surface (7) and locus of the extrema of the principal curvatures along their principal directions

$$T(x^1, x^2, x^3) = \frac{dk_{\max}}{ds_{\max}} \cdot \frac{dk_{\min}}{ds_{\min}} = 0, \quad (15)$$

where the derivatives are given by (9). The quantity T is called the *Gaussian extremality* and was introduced in [18]. Our numerical experiments confirm remarkable stability properties of the zero crossings of the Gaussian extremality observed in [18].

Tracing the intersection curve of (7) and (15), we extract the ridges according to (14).

We describe below an algorithm of obtaining piecewise linear approximation of the intersection curve for further visualization and analysis.

There are two main numerical approaches to implicit surface-surface intersection:

1. Start with some intersection point found analytically or numerically. Trace the intersection curve by differential equation solving. See, for example, [9].
2. Approximate both surfaces by polygons and intersect two obtained polyhedrons.

Note that these methods treat both surfaces equally. On the other hand, one could observe from the previous sections that even for a simple surface the function defining its ridges can be very complex. It means that evaluation times for these two functions can differ drastically. Therefore, an algorithm aiming to decrease the number of evaluations of the more complex function can substantially decrease the overall computation time.

We propose an alternative intersection method based on the extension of existing implicit surface polygonization algorithms. The idea is to adaptively polygonize the initial surface near the intersection curves and to test the obtained polygons against another surface. If at least one vertex of the polygon lies inside the second surface, endpoints of a segment of the intersection line can be calculated.

The proposed algorithm is based on our implicit surface polygonization method [15] and includes the following steps:

- Define the surface by $F(x^1, x^2, x^3) = 0$ and the the zero crossings of the Gaussian extremality (15), which can be considered as an equation of a trimming surface.
- Introduce a sparse spatial grid in (x^1, x^2, x^3) space.
- Calculate F values at the grid points.
- Obtain the initial triangulation for the surface $F = 0$ following the algorithm [15].

- For each triangle calculate T values in its vertices and check the following adaptation criteria:
 1. Different signs of the function T values in the vertices: the triangle intersects the trimming surface;
 2. Evaluate T in the barycenter of the triangle. If the sign is different from the signs in the vertices, the trimming surface penetrates the triangle but all vertices are outside or inside the surface.
 3. If the absolute value of T is less than some given ε , the triangle is close to the trimming surface with possible surface-surface intersection.
- If one of the adaptation criteria is satisfied, start recursive subdivision of the triangle in four triangles by introducing new vertices in the middle of its edges. Place newly introduced vertices on the initial surface using a search in the normal direction. Repeat the previous step for the four new triangles.
- If none of the adaptation criteria is satisfied for the current triangle or the given level of subdivision is achieved, check the values of the function T in the vertices. If the values have different signs, the endpoints of the intersection line segment can be found by the linear interpolation along the corresponding edges.
- For the purpose of visualization, we extract not only the intersection line segment but a stripe by stepping from each endpoint in both directions along the corresponding triangle edge.

Note that the proposed algorithm starts with the sparse mesh and then invokes its adaptation in the neighborhood of the intersection curve. Moreover, the function T defining the ridges is evaluated only in the vertices of the initial surface mesh but not in the 3D grid points. This helps to decrease the number of time-consuming function evaluations while providing required accuracy of the intersection line extraction.

Experimental results

We test our algorithms on the rounded octahedron

$$F(x, y, z) \equiv x^4 + y^4 + z^4 + 5x^2y^2 + 5y^2z^2 + 5z^2x^2 - 1 = 0.$$

It is a convex surface and we choose the orientation such that both the principal curvatures are positive. Fig. 2 demonstrates intersection between the rounded octahedron $F(x, y, z) = 0$ and the surface of the extrema of the principal curvatures along their principal directions $T(x, y, z) =$

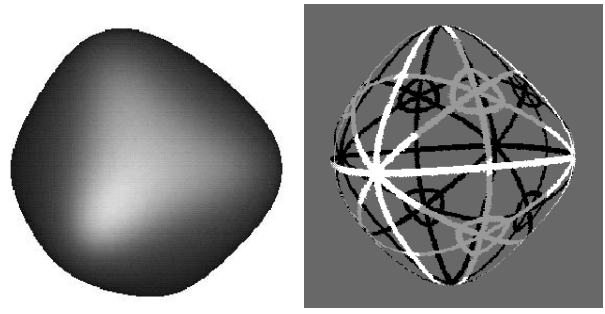


Figure 2.

0. The ridges consisting of the maxima of the maximal principal curvature along the associated curvature line are colored in white.

The initial sparse mesh has $12 \times 12 \times 12$ nodes with four levels of recursion. The processing time is 140 seconds. It gives approximately 70 times speed-up if compared with 2.5 hours of calculation time for the non-adaptive run with equivalent $190 \times 190 \times 190$ resolution.

Although extraction of the ridges on the rounded octahedron according to the approach developed in this paper allows an analytical solution, it exceeds the current possibilities of Maple and Mathematica computer algebra systems. A different approach allowing to extract the ridges analytically (with a computer algebra system) from implicit polynomial surfaces was recently proposed in [3]. In our numerical calculations we use finite differences to approximate derivatives of F .

For robust extraction of the ridges and ravines from real data given in implicit form (isosurfaces of 3D images), preliminary smoothing of the data is required. However smoothing modifies the surface curvature phenomena. A possible remedy lies in adaptive smoothing based on local curvature estimation. This research is in progress now.

Conclusion

We derived formulas to detect the ridges and ravines on a surface given in implicit form. We also proposed and implemented an algorithm of the piecewise linear approximation of ridges and ravines as intersection curves of two implicit surfaces. The algorithm takes into account that the time consuming evaluation of the function defining ridges on the initial surface. The proposed adaptive solution significantly accelerates the ridges/ravines construction.

Acknowledgments

It is our pleasure to acknowledge fruitful discussions with I. A. Bogaevski. We would like to thank referees for

their helpful comments and suggestions. Thanks also to Maple for its help in performing many formal computations presented in the paper. This work was supported in part by the MOVE (Multimedia Open network and Virtual reality for new Education) consortium. The support is gratefully acknowledged.

References

- [1] A. G. Belyaev, E. V. Anoshkina, and T. L. Kunii. Ridges, ravines and singularities. In A. T. Fomenko and T. L. Kunii, *Topological modeling for visualization*, Chapter 18, 1997.
- [2] A. G. Belyaev, I. A. Bogaevski, and T. L. Kunii. Ridges and ravines on a surface and segmentation of range images. In R. A. Melter, A. Y. Wu, and L. J. Latecki, editors, *Vision Geometry VI, Proc. SPIE 3168*, pages 106–114, San-Diego, CA, July 1997.
- [3] I. A. Bogaevski, V. Lang, A. G. Belyaev, and T. L. Kunii. Color ridges on implicit polynomial surfaces. Technical Report 96-1-014, The University of Aizu, Japan, November 1996.
- [4] F. L. Bookstein and C. B. Cutting. A proposal for the apprehension of curving craniofacial form in three dimensions. In K. Vig and B. A., editors, *Craniofacial Morphogenesis and Dysmorphogenesis*, pages 127–140, Center of Human Growth, University of Michigan, Ann Arbor, 1988.
- [5] J. Declerck, G. Subsol, J.-P. Thirion, and N. Ayache. Automatic retrieval of anatomical structures in 3d medical images. Rapport de Recherche 1881, INRIA, Le Chesnay, France, 1995.
- [6] D. Eberly. “MAGIC”, an object-oriented library for image analysis. <http://www.cs.unc.edu/~eberly/>.
- [7] D. Eberly. *Ridges in Image and Data Analysis*. Kluwer, 1996.
- [8] G. G. Gordon. Face recognition from depth maps and surface curvature. In *Geometric Methods in Computer Vision, Proc. SPIE 1570*, pages 234–247, San-Diego, CA, July 1991.
- [9] M. Hosaka. *Modeling of Curves and Surfaces in CAD/CAM*. Springer, Berlin, 1992.
- [10] T. Maekawa and N. M. Patrikalakis. Interrogation of differential geometry properties for design and manufacture. *The Visual Computer*, 10(4):216–237, 1994.
- [11] T. Maekawa, F.-E. Wolter, and N. M. Patrikalakis. Umbilics and lines of curvature for shape interrogation. *Computer Aided Geometric Design*, 13:133–161, 1996.
- [12] G. Medioni and R. Nevatia. Description of 3-d surfaces using curvature properties. In *Proc. DARPA Image Understanding Workshop*, pages 291–299, New Orleans, October 1984.
- [13] O. Monga, N. Armande, and P. Montesinos. Thin nets and crest lines: application to satellite data and medical images. Rapport de Recherche 2480, INRIA, Le Chesnay, France, 1995.
- [14] O. Monga and S. Benayoun. Using partial derivatives of 3d images to extract typical surface features. *Computer Vision and Image Understanding*, 61:171–189, March 1995.
- [15] A. Pasko, V. Pilyugin, and V. Pokrovskiy. Geometric modeling in the analysis of trivariate functions. *Computers and Graphics*, 12(3/4):457–465, 1988.
- [16] I. R. Porteous. *Geometric Differentiation for the Intelligence of Curves and Surfaces*. Cambridge University Press, Cambridge, 1994.
- [17] E. C. Sherbrooke, N. M. Patrikalakis, and F.-E. Wolter. Differential and topological properties of medial axis transform. *Graphical Models and Image Processing*, 58(6):574–592, 1996.
- [18] J. Thirion. The extremal mesh and the understanding of 3d surfaces. *IJCV*, 19(2):115–128, August 1996.
- [19] J.-P. Thirion and A. Gourdon. The marching lines algorithm: new results and proofs. Rapport de Recherche 1881, INRIA, Le Chesnay, France, April 1993.
- [20] G. Turkiyyah, D. Storti, M. Ganter, H. Chen, and M. Vismawala. An acceleration triangulation method for computing the skeletons of free-form solid models. *Computer-Aided Design*, 29(1):5–19, 1997.
- [21] A. Yuille. Zero crossings on lines of curvature. *CVGIP*, 45(1):68–87, January 1989.
- [22] A. Yuille and M. Leyton. 3d symmetry-curvature duality theorems. *CVGIP*, 52(1):124–140, October 1990.